J Neurophysiol 94: 3872–3883, 2005.
First published August 10, 2005; doi:10.1152/jn.00389.2005.

Suppression of I_h Contributes to Propofol-Induced Inhibition of Mouse Cortical Pyramidal Neurons

Xiangdong Chen,[1] Shaofang Shu,[1] and Douglas A. Bayliss[1,2]
[1]*Departments of Pharmacology and* [2]*Anesthesiology, University of Virginia, Charlottesville, Virginia*

Submitted 15 April 2005; accepted in final form 4 August 2005

Chen, Xiangdong, Shaofang Shu, and Douglas A. Bayliss. Suppression of I_h contributes to propofol-induced inhibition of mouse cortical pyramidal neurons. *J Neurophysiol* 94: 3872–3883, 2005. First published August 10, 2005; doi:10.1152/jn.00389.2005. The contributions of the hyperpolarization-activated current, I_h, to generation of rhythmic activities are well described for various central neurons, particularly in thalamocortical circuits. In the present study, we investigated effects of a general anesthetic, propofol, on native I_h in neurons of thalamus and cortex and on the corresponding cloned HCN channel subunits. Whole cell voltage-clamp recordings from mouse brain slices identified neuronal I_h currents with fast activation kinetics in neocortical pyramidal neurons and with slower kinetics in thalamocortical relay cells. Propofol inhibited the fast-activating I_h in cortical neurons at a clinically relevant concentration (5 μM); inhibition of I_h involved a hyperpolarizing shift in half-activation voltage ($\Delta V1/2$ approximately -9 mV) and a decrease in maximal available current (~36% inhibition, measured at -120 mV). With the slower form of I_h expressed in thalamocortical neurons, propofol had no effect on current activation or amplitude. In heterologous expression systems, 5 μM propofol caused a large shift in $V1/2$ and decrease in current amplitude in homomeric HCN1 and linked heteromeric HCN1–HCN2 channels, both of which activate with fast kinetics but did not affect $V1/2$ or current amplitude of slowly activating homomeric HCN2 channels. With $GABA_A$ and glycine receptor channels blocked, propofol caused membrane hyperpolarization and suppressed action potential discharge in cortical neurons; these effects were occluded by the I_h blocker, ZD-7288. In summary, these data indicate that propofol selectively inhibits HCN channels containing HCN1 subunits, such as those that mediate I_h in cortical pyramidal neurons—and they suggest that anesthetic actions of propofol may involve inhibition of cortical neurons and perhaps other HCN1-expressing cells.

INTRODUCTION

Propofol (2,6 di-isopropylphenol) is an intravenous anesthetic with a chemical structure distinct from any other anesthetic that has been gaining use for induction and maintenance of anesthesia in clinical practice during the last 10 yr. Despite this growth in popularity as an anesthetic compound, its mechanisms of action remain incompletely understood. Effects of intravenous anesthetics, including propofol, are generally thought to be mediated by GABAergic mechanisms (Rudolph and Antkowiak 2004; Trapani et al. 2000). Indeed propofol-induced suppression of the withdrawal response to painful stimuli (i.e., its immobilizing action) was completely abolished in mice with a point mutation (N265M) engineered into the β3 subunit of the $GABA_A$ receptor to remove its sensitivity to propofol (Jurd et al. 2003). Interestingly, although recovery from propofol-induced loss-of-righting reflex was accelerated in the β3(N265M) animals (Jurd et al. 2003), the loss-of-righting reflex itself was not blocked. This indicates that the direct hypnotic actions of the drug were relatively preserved in these $GABA_A$ receptor knock-in mice (Jurd et al. 2003). The results with this mouse model are consistent with earlier pharmacological studies, which demonstrated that only the immobilizing, but not the hypnotic, effects of propofol are sensitive to systemic administration of $GABA_A$ receptor blockers (Little et al. 2000; Sonner et al. 2003b).

Additional evidence indicates that propofol can mediate other clinically relevant actions independent of the $GABA_A$ receptor, perhaps via alternative ionic mechanisms. For example, anticonvulsant actions of propofol, assayed as the ability of the drug to reduce epileptiform activity in rat hippocampal slices, are insensitive to the $GABA_A$ receptor antagonist bicuculline (Ohmori et al. 2004). Anesthetic and anticonvulsant properties of propofol have been attributed to suppressive effects on a hyperpolarization-activated cationic current (I_h) in hippocampal pyramidal neurons (Funahashi et al. 2001; Higuchi et al. 2003). In addition, a recent study indicates that propofol can enhance inhibitory input onto thalamocortical relay neurons, gating sensory activity through the thalamus, by blocking small conductance calcium-activated potassium (SK) channels in reticular thalamic neurons (Ying and Goldstein 2005). Thus the overall actions of propofol may involve modulation of ion channels in addition to $GABA_A$ receptors.

There is little detailed information as to which brain regions are critical for different endpoints of anesthesia, but direct or indirect depression of neurons in thalamocortical loops may provide a point of convergence for anesthetic actions, contributing to a sleep-like hypnotic state (Alkire et al. 2000). The pacemaker current, I_h, figures prominently in the firing behavior of neurons in thalamocortical circuits (Pape 1996; Pape and McCormick 1989), where it promotes spontaneous rhythmic activity like that associated with sleep states (Pape 1996). We have demonstrated that native I_h is strongly modulated by volatile anesthetics in motoneurons (Sirois et al. 1998, 2002), cells that are implicated in anesthetic-induced immobilization (Sonner et al. 2003a). In addition, propofol inhibits I_h in hippocampal pyramidal neurons and in the area postrema (Funahashi et al. 2004; Higuchi et al. 2003). This suggests that the channels underlying I_h may represent a point of convergence for multiple classes of anesthetics in various neuronal groups associated with anesthetic actions.

Address for reprint requests and other correspondence: X. Chen, Dept. of Pharmacology, University of Virginia Health System, P.O. Box 800735, 1300 Jefferson Park Ave., Charlottesville, Virginia 22908-0735 (E-mail: xc9b@virginia.edu).

The costs of publication of this article were defrayed in part by the payment of page charges. The article must therefore be hereby marked "*advertisement*" in accordance with 18 U.S.C. Section 1734 solely to indicate this fact.

It is now clear that HCN channels represent the molecular basis for native I_h (Ludwig et al. 1998; Santoro et al. 1997). The four different HCN subunits exhibit distinct biophysical properties, and all are expressed to some degree in the mammalian CNS (Monteggia et al. 2000; Moosmang et al. 1999; Santoro et al. 2000). Among these subunits, HCN1 and HCN2 are most prominently expressed in the CNS, with the HCN1 subunit more selectively localized than HCN2. In the studies reported here, we examined effects of propofol on native I_h in mouse thalamocortical and cortical neurons and on cloned HCN subunits (mHCN1 and mHCN2) expressed heterologously. We find that propofol selectively inhibits fast HCN1 subunit-containing channels, like those that mediate I_h in cortical pyramidal neurons, but does not diminish slower HCN2 channel currents, such as those in thalamocortical neurons.

METHODS

Patch-clamp recordings from thalamic relay and cortical pyramidal neurons

Transverse brain slices from mice and rats of either sex (14–22 days old) were prepared as described previously (Sirois et al. 1998; Talley et al. 2000). Animals were decapitated under ketamine/xylazine anesthesia. The brain was rapidly removed from the cranium and submerged in an ice-cold substituted Ringer solution bubbled with 95% O_2-5% CO_2. The substituted Ringer solution contained (in mM) 260 sucrose, 3 KCl, 5 $MgCl_2$, 1 $CaCl_2$, 1.25 NaH_2PO_4, 26 $NaHCO_3$, 10 glucose, and 1 kynurenic acid (Aghajanian and Rasmussen 1989). Slices (200–300 μm) were cut using a microslicer (DSK 1500E; Dosaka, Tokyo, Japan). Before recording, slices were incubated at 37°C for 1 h and then subsequently at room temperature in a normal Ringer solution (mM) 130 NaCl, 3 KCl, 2 $MgCl_2$, 2 $CaCl_2$, 1.25 NaH_2PO_4, 26 $NaHCO_3$, and 10 glucose, bubbled with 95% O_2-5% CO_2.

Patch-clamp electrodes were pulled from borosilicate glass (Warner Instruments) to a DC resistance of 3–5 MΩ and coated with silicone elastomer (Sylgard 184; Dow Corning). Whole cell recordings were obtained from visually identified pyramidal neurons in layer V of somatosensory cortex and from relay neurons in the ventrobasal thalamic nucleus by using infrared differential interference contrast (IR-DIC) microscopy (Zeiss Axioskop FS Plus) and an Axoclamp 200B amplifier (Axon Instruments). Cell capacitance and series resistance (R, typically <20 MΩ) were compensated using the amplifier circuits (typically ~70% R compensation). In addition, R was continuously monitored on an oscilloscope between test pulses by using the seal test function on the amplifier. Only cells with stable R were included and any small changes in R were corrected on-line by using the compensation circuits of the amplifier.

For voltage-clamp recordings, the pipette solution contained (in mM) 120 KCH_3SO_3, 4 NaCl, 1 $MgCl_2$, 0.5 $CaCl_2$, 10 HEPES, 10 EGTA, 3 MgATP, and 0.3 GTP-Tris, pH 7.2 and 280 mosM. Current-clamp recordings were made with pipette solution containing (in mM) 17.5 KCl, 122.5 potassium gluconate, 1 $MgCl_2$, 9 NaCl, 10 HEPES, 0.2 EGTA, 3 Mg-ATP, and 0.3 Tris-GTP, pH 7.2 and 272 mosM. Recordings were obtained at room temperature (22–24°C) while slices were continuously superfused (~3–4 ml/min) with a solution containing (mM) 140 NaCl, 3 KCl, 2 $MgCl_2$, 2 $CaCl_2$, 10 HEPES and 10 glucose, pH 7.3. The properties of neuronal I_h (i.e., maximal amplitude, voltage dependence) measured in slices using a HEPES-based bath solution equilibrated with room air (i.e., 21% O_2) are virtually identical to those obtained with a hyperoxic HEPES bath solution (100% O_2) or with normal Ringer solution bubbled with 95% O_2-5% CO_2 (data not shown). All data were corrected for a measured liquid junction potential of 8 mV.

To block I_h in some experiments, ZD-7288 (50 μM; Tocris Cookson) was included in the pipette solution or CsCl was added to the bath (3 mM). We also included $BaCl_2$ (200 μM) in most voltage-clamp experiments to inhibit inwardly rectifying K^+ currents in cortical and thalamic neurons. Where noted, tetrodotoxin (TTX at 0.5 μM, Alomone Labs) was added to the perfusate to block action potentials and a bicuculline/strychnine cocktail (both at 30 μM; from Sigma) was added to block $GABA_A$ and glycine receptor channels. Propofol (Sigma, St. Louis, MO) was prepared as a 100 mg/ml stock solution in ethanol and diluted in bath solution to the indicated concentrations; propofol was applied to neurons in the slice for ~5 min [5.1 ± 0.5 (SD) min], a point at which we found inhibition of I_h in cortical neurons was stable and maximal. In a subset of experiments on thalamocortical cells, propofol was perfused for 20 min before effects on I_h were assessed.

Voltage-clamp recording of heterologously expressed mHCN channels

We obtained mHCN1 and mHCN2 from Drs. B. Santoro and S.A. Siegelbaum (Columbia University). The concatemeric HCN1–HCN2 construct was made by using overlap extension PCR to produce a *Psh*AI-*Nhe*I fragment that spliced the final leucine of HCN1 directly in frame with the initiating methionine of HCN2 (Chen et al. 2005). The pGHE vector was used for oocyte expression and the pcDNA3 vector for expression in mammalian cells.

To prepare RNA for injection, in vitro transcription was performed with *Nhe*I-linearized DNA (HCN1), *Sph*I-linearized DNA (HCN2), or *Xba*I-linearized DNA (HCN1–HCN2) using T7 RNA polymerase (Message Machine; Ambion, Houston, TX). *Xenopus laevis* oocytes (obtained from Drs. G. Kamatchi and H. Fang, University of Virginia) were injected with 46 nl of RNA (50–200 ng/μl) using a Nanoject microinjector (Drummond Scientific). After injection, oocytes were incubated at 17°C for 1–3 days in ND-96 solution, containing (in mM) 96 NaCl, 2 KCl, 1.8 $CaCl_2$, 1 $MgCl_2$, and 5 HEPES, pH 7.5, that was supplemented with 5% (wt/vol) gentamycin sulfate. Whole cell currents were recorded from oocytes in solution, containing (in mM) 107 KCl, 5 NaCl, 10 HEPES, 1 $MgCl_2$, and 1 EGTA, pH 7.3, at room temperature with the two-microelectrode voltage-clamp technique using a Warner OC-725B amplifier (Warner Instruments, Hamden, CT). Voltage recording and current injecting electrodes were filled with 3 M KCl (1–3 MΩ).

HEK 293 cells were cultured using standard procedures and transiently transfected with HCN channel constructs, together with a GFP plasmid (pGreenLantern; GIBCO) using Lipofectamine 2000 reagent (Invitrogen). After transfection (1–2 days), whole cell recordings of HCN channel currents were obtained from HEK293 cells as described in the preceding text for neuronal recordings, except that the bath KCl concentration was raised to 25 mM (substituted equimolar for NaCl) (also see Chen et al. 2005).

Data acquisition and analysis

Data were acquired using pCLAMP software (Axon Instruments) and a Digidata 1322A or a Digidata 1200 digitizer (Axon Instruments). For voltage-clamp recording, time-dependent hyperpolarization-activated currents (I_h, HCN) were evoked with incrementing (Δ −10 mV) hyperpolarizing pulses (3–4 s) from a holding potential of −40 or −50 mV, followed immediately by a step to fixed potential (−90 or −100 mV) to obtain tail currents. Current amplitude at each potential was taken as the difference between "instantaneous" currents, measured immediately after the capacitive transient, and the current at the end of hyperpolarizing voltage steps; maximal available current was determined at −120 or −130 mV. Tail currents were normalized, plotted as a function of the preceding hyperpolarization step voltage and fitted with Boltzmann curves for derivation of half-activation voltage ($V1/2$) by using a least squares analysis and the

"solver" add-in of Excel (Microsoft). Time constants (τ) were determined by fitting currents evoked during hyperpolarizing steps to a biexponential function. Results are presented as means ± SE. Data were analyzed statistically using one-way ANOVA or Students *t*-test, as indicated; post hoc pairwise comparisons used Bonferroni's correction of the *t*-test (Excel or SigmaStat). Differences in mean values were considered significant if $P < 0.05$.

Histology

In all slice experiments, 0.2% biocytin (Sigma-Aldrich) was included in the patch electrode solution for subsequent morphological identification of recorded cells. Slices were fixed in 4% buffered paraformaldehyde solution for ≥24 h and then rinsed and incubated for 30 min with 1% H_2O_2 and for 30 min with 0.5% Triton X-100. A 2-h incubation with avidin-biotin complex was followed by incubation in a diaminobenzidine substrate kit (both from Vector Labs, Burlingame, CA). Finally, slices were mounted onto gelatin-subbed slides and left to air dry overnight. Slices were dehydrated through graded ethanol and xylene and embedded in DPX mounting medium (BDH Laboratory Supplies); biocytin-stained neurons were visualized and photographed using an Axioskop microscope (Zeiss), equipped with a digital camera (Retiga 1300C, QImaging) and IPLab software (Scanalytics).

RESULTS

Propofol differentially modulates native I_h in neocortical pyramidal neurons and thalamocortical neurons

We used whole cell patch-clamp recording in mouse brain slices to characterize hyperpolarization-activated currents (I_h) and their modulation by propofol in thalamocortical and neocortical neurons. Representative examples of cell morphology and I_h recorded from those neurons are depicted in Fig. 1. In a multipolar thalamocortical neuron from the ventral posteromedial nucleus (Fig. 1*A*), currents evoked by hyperpolarizing voltage steps activated in a voltage-and time-dependent manner as expected of I_h. In pyramidal neurons from somatosensory cortex (Fig. 1*B*), I_h was also observed during hyperpolarizing voltage steps; in cortical neurons, however, I_h activated with faster kinetics than in thalamocortical neurons. Biexponential fits to I_h obtained at fixed membrane potential of −120 mV revealed a variable slow component of I_h that was accompanied by a fast component that accounted for the majority of current in both cortical and thalamocortical neurons (>60%). In most cortical neurons, I_h activated with a fast time constant (τ_f) that was <200 ms (τ_f = 79.5 ± 14.2 ms; n = 9 of 12 cortical neurons recorded). Activation kinetics were much slower (τ_f >200 ms at −120 mV) in a subpopulation of cortical neurons (τ_f = 434.6 ± 16.2 ms; n = 3) and in all thalamic neurons (τ_f = 338.9 ± 32.1 ms; n = 10).

These distinct kinetic properties of I_h typical of cortical and thalamic neurons are consistent with earlier recordings of I_h from these two brain regions and with known patterns of HCN subunit expression in mouse cortex and thalamus (e.g., see Santoro et al. 2000). In neocortical neurons, there is relatively high expression of fast-activating HCN1 subunits and moderate levels of slow-activating HCN2 subunits (Franz et al. 2000; Santoro et al. 2000). In thalamocortical neurons, HCN1 is barely detectable and the slower HCN2 and HCN4 isoforms predominate (Notomi and Shigemoto 2004; Santoro et al. 2000) with the majority of the current (80–90%) attributed to HCN2 (Ludwig et al. 2003).

We found that the intravenous general anesthetic, propofol, acts differently on I_h in cortical and thalamic neurons. As exemplified in records from the representative cells of Fig. 1, propofol (5 μM, for ~5 min) had little effect on I_h in thalamic neurons, but it caused a robust inhibition of I_h in the group of cortical neurons with fast activation kinetics (τ_f <200 ms). The effect of propofol on I_h may be seen more clearly as propofol-sensitive currents (Fig. 1, *right*), which were obtained by subtracting currents in the presence of propofol from those in control conditions. There was essentially no propofol-sensitive current in thalamic neurons, but we observed a substantial propofol-sensitive current with time and voltage dependence characteristic of I_h in cortical neurons.

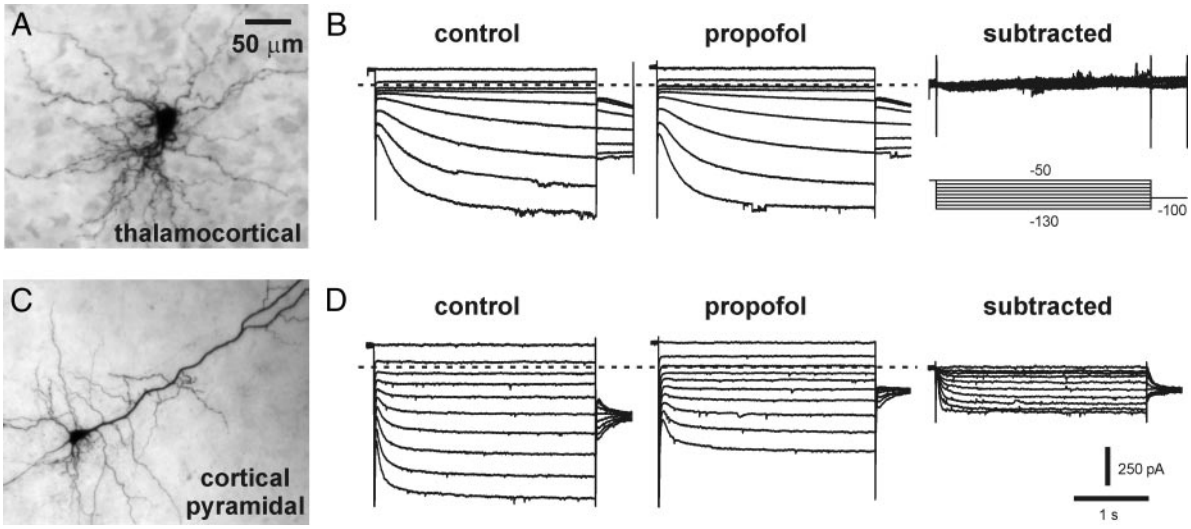

FIG. 1. Propofol inhibits I_h in cortical pyramidal cells but not in thalamocortical relay neurons. *A*: photomicrograph of a biocytin-stained thalamocortical neuron recorded from the ventral posteromedial nucleus. *B*: voltage clamp recordings of I_h (from the cell depicted in *A*) under control conditions (*left*) and in 5 μM propofol (*middle*). Subtracted currents (control − propofol) reveal the propofol-sensitive current (*right*). The voltage-clamp pulse protocol is depicted in the *inset* and is typical of that used throughout these studies (conditioning voltage steps were always 3–4 s in duration). *C*: photomicrograph of a biocytin-stained pyramidal neuron recorded from somatosensory cortex. *D*: voltage-clamp recordings of I_h (from the cell depicted in *C*) under the indicated conditions. Note the slower kinetics of I_h in the thalamic neuron and that propofol only inhibited the faster-activating current in the cortical neuron.

The inhibition by propofol of fast-activating I_h in cortical neurons was manifest in two prominent effects: a shift in voltage dependence of activation and a decrease in maximal available current. As depicted in Fig. 2*A* (*left*), analysis of tail currents evoked at −100 mV after hyperpolarizing voltage steps to different membrane potentials revealed a propofol-induced hyperpolarizing shift in *V*1/2 by −9 ± 0.9 mV (from −94.4 ± 1.0 to 103.6 ± 1.2 mV, $n = 9$, $P < 0.001$). In addition, as shown in *I-V* relationships for I_h in these cortical neurons (Fig. 2*A, right*), propofol reduced maximal time-dependent current at the end of hyperpolarizing steps to −120 mV by 35.9 ± 5.6% ($P < 0.001$); propofol also decreased input conductance at the holding potential by ~15%, as evident by the decreased slope of averaged "instantaneous" *I-V* curves (from 6.2 ± 0.2 to 5.3 ± 0.2 nS; $P < 0.005$, see Fig. 2*A, inset*). We also noted that current activation kinetics were slowed by propofol (τ_f at −120 mV from 79.5 ± 14.2 to 112.5 ± 26.2 ms, $n = 9$, $P < 0.05$).

By contrast, propofol had no effect on I_h voltage dependence (−98.3 ± 0.6 and −97.8 ± 0.9 mV in control and propofol; Fig. 2*B, left*), amplitude (0.5 ± 0.0% activation; Fig. 2*B, right*) or on input conductance (2.6 ± 0.6 and 2.5 ± 0.5 nS in control and propofol) in thalamic neurons ($n = 5$) or in the group of three cortical neurons with a slow form of I_h (*V*1/2: −101.2 ± 2.2 and −100.1 ± 2.8 mV in control and propofol; amplitude inhibition: 3.7 ± 0.1%). To rule out any concerns with the slow equilibration of propofol in slices (Bieda and MacIver 2004; Gredell et al. 2004), we confirmed that propofol remained without effect on *V*1/2 or maximal amplitude of I_h after a 20-min exposure to propofol (*V*1/2: −103.9 ± 1.2 and −106.4 ± 1.9 mV in control and propofol; amplitude inhibition: 7.6 ± 3.3%; $n = 5$, NS). It is noteworthy, however, that propofol did slow activation kinetics in all thalamocortical cells (τ_f at −120 mV from 338.9 ± 32.2 to 474.1 ± 81.2 ms, $n = 10$, $P < 0.05$), and this effect was fully evident even after only 5 min of propofol application (τ_f at −120 mV from 409.8 ± 39.2 to 637.5 ± 126.1 ms, $n = 5$, $P < 0.05$). These data indicate that although an action of propofol on activation kinetics can be discerned in thalamocortical neurons, the anesthetic does not modulate voltage dependence or maximal amplitude of I_h under conditions identical to those in which the fast activating I_h in cortical neuron is clearly inhibited.

We extended this analysis to motoneurons of the rat hypoglossal nucleus, which like mouse cortical pyramidal neurons, co-express high levels of HCN1 and moderate levels of HCN2 (Chen et al. 2005; Monteggia et al. 2000) and present a relatively fast form of I_h (τ_f at −120 mV: 126.3 ± 9.5 ms, $n = 7$). In these motoneurons, 5 μM propofol caused a hyperpolarizing shift in activation voltage ($\Delta V1/2 = -5.8 \pm 2.3$ mV, from −92.8 ± 2.4 to −98.6 ± 3.7 mV, $P < 0.05$) and a decrease in maximal current amplitude (20.6 ± 6.0% inhibition, $P < 0.05$). Thus propofol modulated the fast-activating I_h observed in rat motoneurons, although not quite as strongly as in mouse cortical neurons (approximately −10 mV shift in *V*1/2 and ~40% inhibition of peak current).

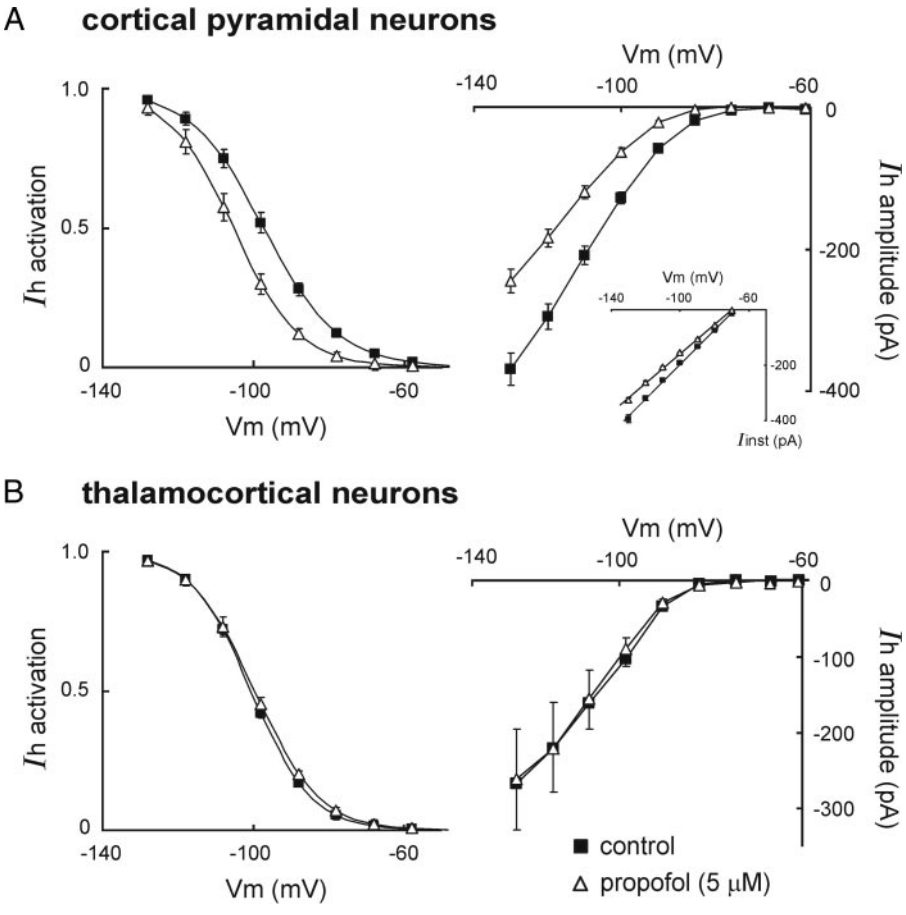

FIG. 2. Modulation of fast-activating I_h in cortical neurons includes a shift in activation gating and a decrease in maximal available current. The effect of propofol was determined on fast-activating I_h (*A*) in cortical pyramidal neurons (τ_f <200 ms at −120 mV; $n = 9/12$ neurons) and on slower-activating I_h (*B*) in thalamocortical neurons (τ_f >200 ms at −120 mV; $n = 5/5$ neurons). Under control conditions (■), and in the presence of propofol (△), normalized tail currents were obtained after incrementing hyperpolarizing steps, averaged and fitted with Boltzmann curves (*left*). Likewise, time-dependent currents were measured at the end of each voltage step in control and propofol and plotted as a function of membrane potential. Propofol induced approximately −9 mV shift in *V*1/2 of I_h activation and ~36% decrease in I_h amplitude (at −120 mV) in cortical neurons but had no effect on I_h in thalamocortical cells. The *inset* in *A* plots "instantaneous" currents evoked by hyperpolarizing voltage steps in cortical neurons, measured immediately after the capacitive transient but before development of the time-dependent current; propofol decreased the slope of the instantaneous *I-V* curve (i.e., the input conductance).

Propofol differentially modulates HCN1 and HCN2 channel subunits at clinically relevant concentrations

The data presented in the preceding text indicate that propofol inhibits current amplitude, slows activation kinetics, and shifts the voltage dependence of fast-activating I_h in mouse cortical neurons but only modulates activation kinetics of the slower I_h recorded from mouse thalamocortical cells. Because fast-activating HCN1 subunits are prominently expressed in cortex and slower-activating HCN2 subunits are predominant in thalamus (Ludwig et al. 2003; Santoro et al. 2000), we considered the possibility that these effects represent differential modulation of channels containing HCN1 and HCN2 subunits.

To test this hypothesis, we recorded currents from cloned mHCN1 and mHCN2 channel subunits expressed in *Xenopus* oocytes (Fig. 3). As reported, these two mHCN subunits produce homomeric channels with different activation properties: mHCN2 currents activate more slowly and at more hy-

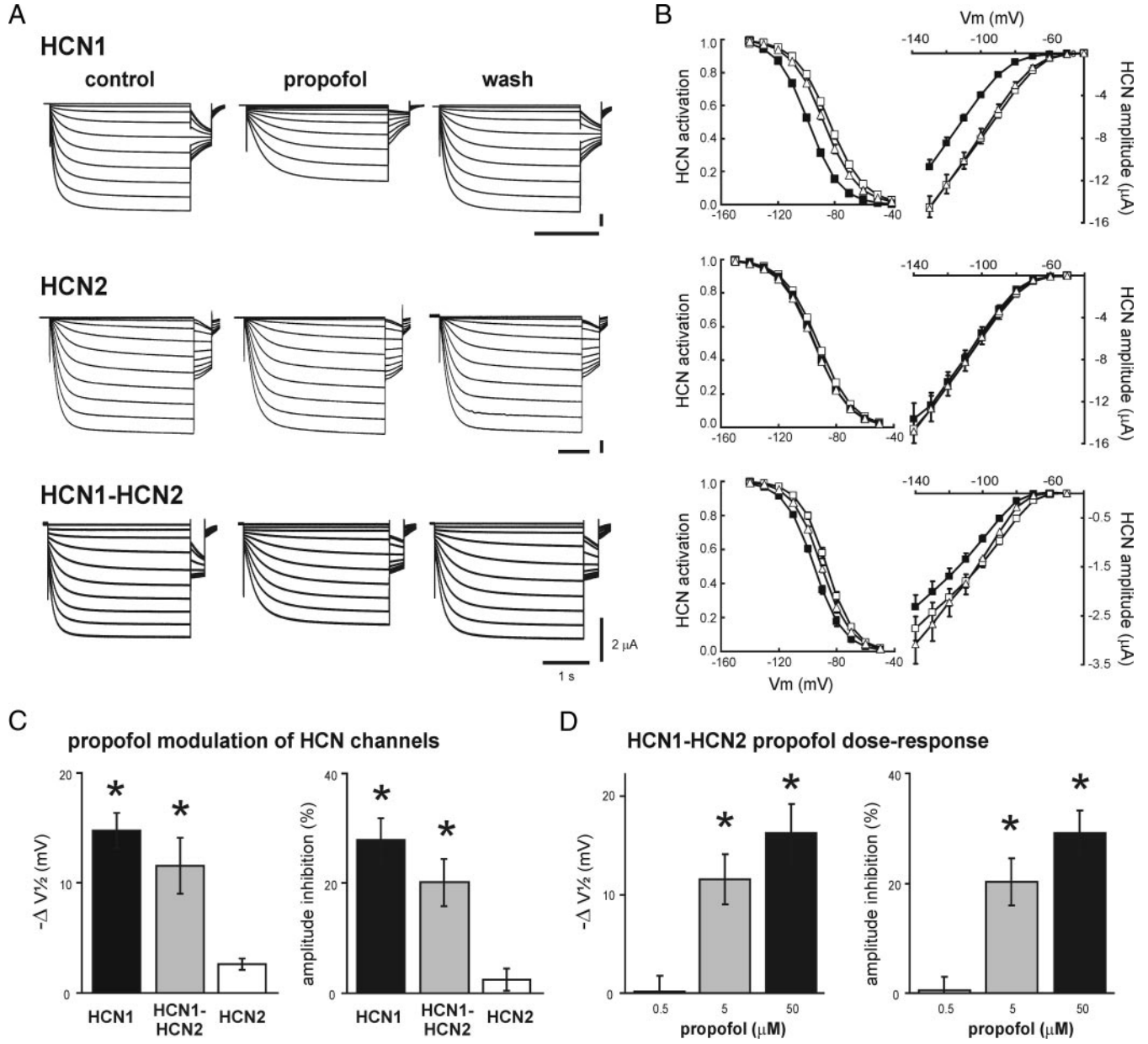

FIG. 3. Propofol modulates HCN channels containing the mHCN1 subunit. *A*: sample currents from *Xenopus* oocytes expressing mHCN1, mHCN2, or a tandem-linked heteromeric mHCN1–HCN2 construct evoked by hyperpolarizing voltage steps from −40 to −130 mV before, during, and after exposure to propofol (5 μM); conditioning voltage steps were of different duration for the three constructs (2, 3, and 4 s for HCN1, HCN1–HCN2, and HCN2, respectively) and followed by a step to −90 mV for tail current analysis. *B*: activation curves were fitted according to the Boltzmann equation to normalized, averaged tail currents (*left*) and averaged steady-state *I-V* curves were obtained from currents at the end of the voltage steps (*right*) under control conditions (□), during exposure to 5 μM propofol (■) and after recovery (△) for HCN1, HCN2. or a linked HCN1–HCN2 construct. *C*: effect of propofol (5 μM) on half-activation potential ($\Delta V1/2$) and maximal current amplitude was determined in individual oocytes expressing the indicated constructs under control conditions and averaged (±SE, $n = 7$, 8 and 6 for HCN1, HCN2, and HCN1–HCN2). *, significantly different from HCN2, $P < 0.05$ by ANOVA. *D*: concentration-response data for propofol (0.5, 5 and 50 μM) modulation of HCN1–HCN2 heteromeric channel currents in oocytes; a significant hyperpolarizing shift in *V*1/2 (*left*) and inhibition of current amplitude (*right*) were already evident at only 5 μM propofol. *, significantly different from 0.5 μM, $P < 0.05$ by ANOVA.

perpolarized potentials than mHCN1 currents (Biel et al. 1999; Kaupp and Seifert 2001; Santoro and Tibbs 1999). We found that channels containing these subunits also differed in their modulation by propofol. In oocytes expressing mHCN1 subunits, propofol (5 μM) caused a hyperpolarizing shift in voltage dependence of activation ($\Delta V1/2$ of -14.8 ± 1.6 mV, from -86.3 ± 2.2 to -100.6 ± 1.3 mV, $n = 6$, $P < 0.005$) and a decrease in maximal current amplitude of $27.9 \pm 4.0\%$ ($P < 0.05$; Fig. 3*C*). These effects are similar to those observed on native I_h in cortical neurons. On the other hand, propofol induced little effect on voltage dependence or amplitude of mHCN2 channel currents expressed in oocytes ($V1/2$: -94.4 ± 3.6 and -96.8 ± 3.5 mV in control and propofol; amplitude inhibition: $2.5 \pm 2.0\%$; Fig. 3*C*). For both mHCN1 and mHCN2, propofol caused a slowing of current activation (τ_f at -120 mV from 66.0 ± 4.4 to 238.2 ± 16.1 ms, $n = 5$; and from 304.6 ± 35.2 to 438.0 ± 71.0 ms, $n = 5$; both $P < 0.05$).

These data indicate that the intravenous anesthetic propofol differentially inhibits HCN1 and HCN2 homomeric channels expressed in *Xenopus* oocytes. We confirmed these results in a mammalian expression system. In HEK293 cells expressing HCN1 channels, propofol shifted $V1/2$, decreased current amplitude and slowed activation kinetics ($\Delta V1/2$: -20.5 ± 1.7 mV; amplitude inhibition: $16.5 \pm 4.1\%$; τ_f at -120 mV from 22.4 ± 5.5 to 106.8 ± 9.4 ms; $n = 7$, all $P < 0.05$); these effects of propofol on HCN1 channels were significantly greater than on HCN2-expressing cells ($\Delta V1/2$: -5.0 ± 0.4 mV; amplitude inhibition: $2.5 \pm 2.8\%$; $n = 9$, $P < 0.05$), except for the slowing of current activation that was again prominent with HCN2 channels in HEK293 cells (τ_f at -120 mV from 225.8 ± 29.1 to 335.1 ± 50.8 ms; $n = 8$, $P < 0.01$). We have reported that distinct inhibitory effects of an inhaled anesthetic, halothane, on HCN1 and HCN2 homomeric channels reflect different basal properties of the channels that can be overcome by cAMP modulation (Chen et al. 2005). However, addition of saturating cAMP (50 μM) to pipettes used to record HCN2 currents in HEK293 cells did not enhance propofol effects on either $V1/2$ or current amplitude (data not shown, $n = 5$). Thus cAMP did not uncover additional latent inhibition of HCN2 channels by propofol.

Propofol inhibits heteromeric HCN1–HCN2 channels

A number of previous studies have demonstrated that HCN subunits can form heteromeric channels (Chen C. et al. 2001; Much et al. 2003; Ulens and Tytgat 2001). Therefore we prepared a linked mHCN1 and mHCN2 cDNA and expressed that construct in oocytes to test effects of propofol on heteromeric HCN channels (Fig. 3). By using this concatenated construct, we were able to record from a homogenous population of HCN1–HCN2 heterotetrameric channels with a defined 1:1 stoichiometry; this approach yields macroscopic currents nearly identical to those obtained by co-injecting HCN1 and HCN2 subunit mRNAs in equal proportions (Chen C. et al. 2001; Ulens and Tytgat 2001).

As expected, we found that the linked HCN1–HCN2 heteromeric channel currents displayed kinetic and voltage-dependent properties intermediate to those of homomeric mHCN1 and mHCN2 channels (Fig. 3, *A* and *B*) (Chen C. et al. 2001; Ulens and Tytgat 2001). Likewise, effects of propofol on linked mHCN1–HCN2 heteromeric channel currents were also intermediate between those of mHCN1 and mHCN2 channels, inducing a hyperpolarizing shift in $V1/2$ of -11.6 ± 2.6 mV (from -88.2 ± 1.3 to -100.2 ± 2.2 mV; $n = 5$, $P < 0.005$) and a decrease of maximal current amplitude by $20.2 \pm 4.3\%$ ($P < 0.05$; Fig. 3*C*); propofol also cause a slowing of HCN1–HCN2 current activation (τ_f at -120 mV from 105.7 ± 6.1 to 215.3 ± 13.6 ms, $n = 5$, $P < 0.005$). Again, we confirmed these results in HEK293 cells expressing HCN1-HCN2 channels ($\Delta V1/2$: -10.2 ± 0.9 mV; amplitude inhibition: $10.6 \pm 3.5\%$; τ_f at -120 mV from 71.5 ± 12.8 to 134.3 ± 16.9 ms; $n = 8$, all $P < 0.05$). Thus effects of propofol on heteromeric HCN channels were also similar to those observed on I_h from most cortical neurons. Moreover, these data indicate that propofol inhibits either homomeric or heteromeric channels that contain HCN1 subunits.

We tested effects of propofol on HCN1-HCN2 heteromeric channels expressed in oocytes over a range of concentrations that encompasses those achieved clinically (0.5–50 μM). Propofol induced a hyperpolarizing shift in the voltage dependence of activation (Fig. 3*D, left*) and suppressed amplitude of heteromeric HCN channel currents (Fig. 3*D, right*) in a dose-dependent manner. There was little effect of propofol at 0.5 μM but a significant shift in $V1/2$ and a decrease in maximal current amplitude both at 5 μM ($\Delta V1/2$: -11.0 ± 1.9 mV; amplitude inhibition: $20.2 \pm 3.1\%$, $n = 6$) and at 50 μM ($\Delta V1/2$: -16.4 ± 1.4 mV; amplitude inhibition: $29.3 \pm 4.3\%$, $n = 5$). These results indicate that propofol inhibits heteromeric HCN channels in dose-dependent manner over a clinically relevant concentration range.

Propofol modulates thalamic and cortical neuron I_h with fast activation kinetics indicative of channels containing HCN1 subunits

A summary of data relating activation kinetics of cloned HCN channels and native neuronal I_h to effects of propofol on voltage dependence of activation and maximal current amplitude is provided in Fig. 4. As described in the preceding text, activation kinetics of native I_h currents in individual neurons and of HCN channel currents expressed in oocytes were analyzed by using biexponential fits to currents obtained at -120 mV. The time constant of the fast exponential component (τ_f) from cortical and thalamic neurons was correlated with both the shift in $V1/2$ and the decrease in maximal current amplitude by propofol in a manner consistent with averaged data from mHCN channel currents expressed in Xenopus oocytes. Thus propofol induced a hyperpolarizing shift in $V1/2$ and inhibition of I_h amplitude in all cells with fast activation kinetics (τ_f <200 ms), including the majority of cortical neurons and oocytes expressing either mHCN1 or mHCN1-2. In all neurons with fast activating I_h, the shift in $V1/2$ and the amplitude inhibition by propofol was greater than the largest effect of propofol in HCN2-expressing oocytes. On the other hand, there was little effect of propofol on $V1/2$ or current amplitude of the slowly activating I_h in thalamic neurons, the response of which resembled that observed in oocytes expressing mHCN2. Note, also, that the few cortical neurons that expressed a slow form of I_h were also relatively insensitive to propofol (Fig. 4, see shaded triangles with τ_f>200 ms). These data indicate that native I_h currents with fast kinetics, presum-

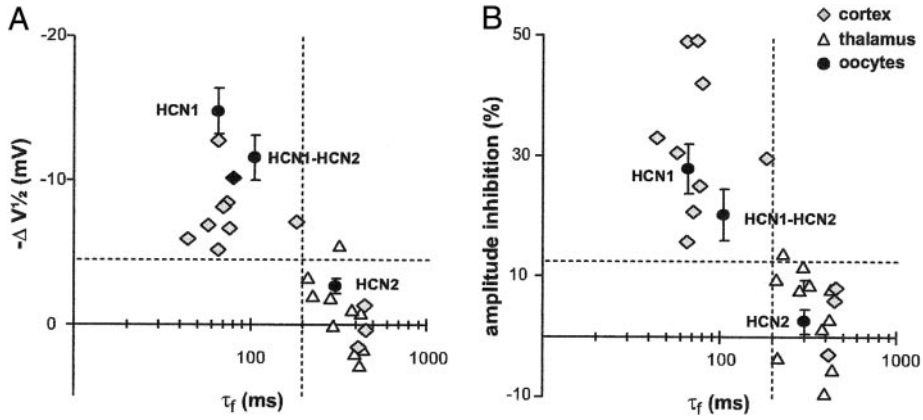

FIG. 4. Propofol modulates fast-activating HCN channels and neuronal I_h. The relationship between activation kinetics of neuronal I_h or HCN currents and the shift in *V1/2* (*A*) or inhibition of maximal current amplitude (*B*) induced by propofol (5 μM). Activation data were obtained from biexponential fits at −120 mV, and the time constant (τ_f) describing the fastest (and largest) current component was plotted together with data from individual neurons or averaged data (±SE) from oocytes expressing the indicated constructs. In most cortical neurons (◆), or in oocytes expressing HCN1 and HCN1–HCN2 channels, currents activated with a τ_f <200 ms (⋮). In these cells, propofol induced a shift in *V1/2* or a current inhibition that was greater than the largest effect measured in all but 1 thalamic neuron (△) or in any HCN2-expressing oocyte (· · · ; $\Delta V1/2$ = 4.5 mV: inhibition = 12.4%). Note that there was little effect of propofol on the three cortical neurons with a slow form of I_h (τ_f >200 ms).

ably those containing HCN1 subunits, are subject to these inhibitory actions of propofol.

Propofol differentially modulates instantaneous HCN channel current

An instantaneous component of current, in addition to the voltage- and time-dependent component, has been observed in recordings from cloned HCN channels (Ludwig et al. 1998; Macri and Accili 2004; Mistrik et al. 2005; Proenza et al. 2002). This current component represents tonic activation of HCN channels at holding potentials depolarized to the threshold for voltage-dependent activation and, at least for HCN2 channels, can represent ~10% of the total available current (Chen et al. J. 2001; Decher et al. 2004). We therefore tested if propofol inhibits instantaneous currents from HCN channels and if it does so in a subunit-specific manner. In HEK293 cells expressing HCN1, HCN2, and HCN1–HCN2, we measured input conductance as the slope of *I-V* relationships from instantaneous currents (i.e., measured immediately after the capacitive transient and before development of time-dependent currents) evoked by hyperpolarizing voltage steps from a holding potential of −40 mV. As is evident in Fig. 5, instantaneous currents generated from all three HCN constructs were inhibited by 3 mM CsCl, an HCN channel blocker. Importantly, and consistent with the differential effects we observed on voltage- and time-dependent HCN currents, propofol inhibited tonically active currents from HCN1 and HCN1–HCN2 channels but had no effect on instantaneous HCN2 channel currents. When expressed relative to the Cs^+-sensitive input conductance (a measure of the tonically-active HCN current), propofol inhibited ~50% of instantaneous HCN1 current, ~30% of instantaneous HCN1–HCN2 current, but only ~5% of the instantaneous HCN2 current. These data confirm earlier observations of tonically active HCN channel currents at depolarized membrane potentials (Ludwig et al. 1998; Macri and Accili 2004; Mistrik et al. 2005; Proenza et al. 2002), and they demonstrate that propofol robustly and preferentially inhibits tonic currents from channels containing HCN1 subunits.

Propofol causes membrane hyperpolarization and decreases excitability in cortical neurons by inhibition of I_h

We next asked, for neocortical neurons where mHCN1 transcripts are prominent and where we observed potent inhibition of I_h by propofol, whether propofol-induced modulation of I_h results in a significant inhibition of cortical neuron excitability. To determine effects of propofol on cell excitability and resting potential, we performed continuous recordings of voltage responses elicited by rectangular depolarizing current injection, in the presence of $GABA_A$ and glycine receptor antagonists (bicuculline and strychnine, both at 30 μM). As shown in Fig. 6 for a representative cortical pyramidal neuron, propofol caused hyperpolarization of resting membrane potential that averaged 4.1 ± 0.1 mV (n = 9), and it decreased cell excitability, even when membrane potential was returned to control levels by DC current injection. On average, propofol increased the current necessary to induce action potential discharge from 0.44 ± 0.02 nA to 0.72 ± 0.02 in 5 μM propofol (n = 5, P < 0.05) and to 0.54 ± 0.02 nA in propofol when membrane potential was returned to control by depolarizing DC current injection.

To confirm that the propofol-induced hyperpolarization of membrane potential was caused by suppression of I_h, we studied cortical neurons with or without ZD-7288 (50 μM), a potent I_h channel antagonist (Bosmith et al. 1993), in the pipette solution (Fig. 7). Again, recordings were performed in the presence of bicuculline and strychnine to block $GABA_A$ and glycine channels. In a cell recorded without ZD-7288 in the pipette (Fig. 7*A, left*), propofol induced a membrane hyperpolarization, as described in the preceding text (approximately −4 mV; see Fig. 7*D,* for averaged data). Propofol also increased input resistance (~9%, from 142.5 ± 5.5 to 154.5 ± 5.9 MΩ; n = 8, P < 0.005) and eliminated the rebound action potential discharge after the hyperpolarizing current pulse (Fig. 7*A, right*). Note that the depolarizing "voltage sag" and rebound potential, which correspond to activation and deactivation of I_h, respectively were not eliminated by propofol. This likely reflects the partial nature of propofol-induced inhibition of I_h as well as enhanced activation of the residual I_h during the

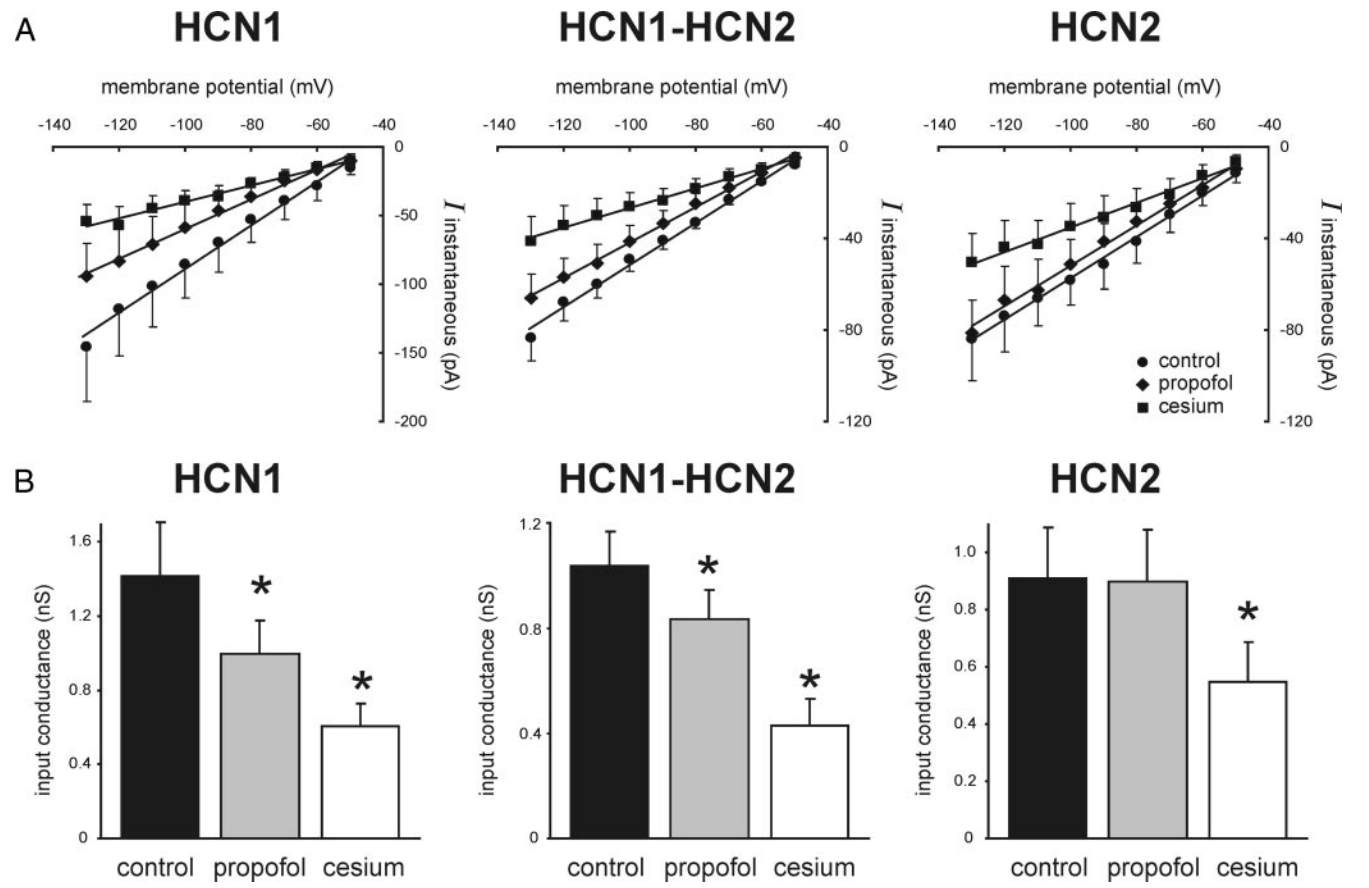

FIG. 5. Propofol inhibits a Cs^+-sensitive instantaneous HCN channel current. *A*: instantaneous *I-V* relationships were obtained from a holding potential of −40 mV in HEK293 cells expressing HCN1 (*left*), HCN1–HCN2 (*middle*), and HCN2 (*right*) under control conditions (●), in the presence of 5 μM propofol (◆), and 3 mM CsCl (■). —, linear fits through averaged data (±SE; $n = 7$, 10, and 9 for HCN1, HCN2, and HCN1–HCN2, respectively), representing the input conductance at −40 mV. *B*: input conductance was determined from instantaneous *I-V* curves in individual cells expressing the HCN channel constructs, and averaged for each condition as indicated. Propofol decreased input conductance in HCN1- and HCN1–HCN2-expressing cells but not in cells expressing HCN2; cesium inhibited the tonic current in all HCN transfected cells (*, $P < 0.05$ vs. control).

current pulse as a result of the membrane hyperpolarization and increased R_N that also accompanied propofol actions.

In cells recorded with 50 μM ZD-7288 in the pipette solution, we observed a time-dependent increase in input resistance (~19%, from 115.1 ± 1.0 to 136.7 ± 2.7 MΩ; $n = 4$, $P < 0.05$) and hyperpolarization of membrane potential (Fig. 6*B, left*) that proceeded for ~5 min after whole cell access; after reaching a steady-state, membrane potential in

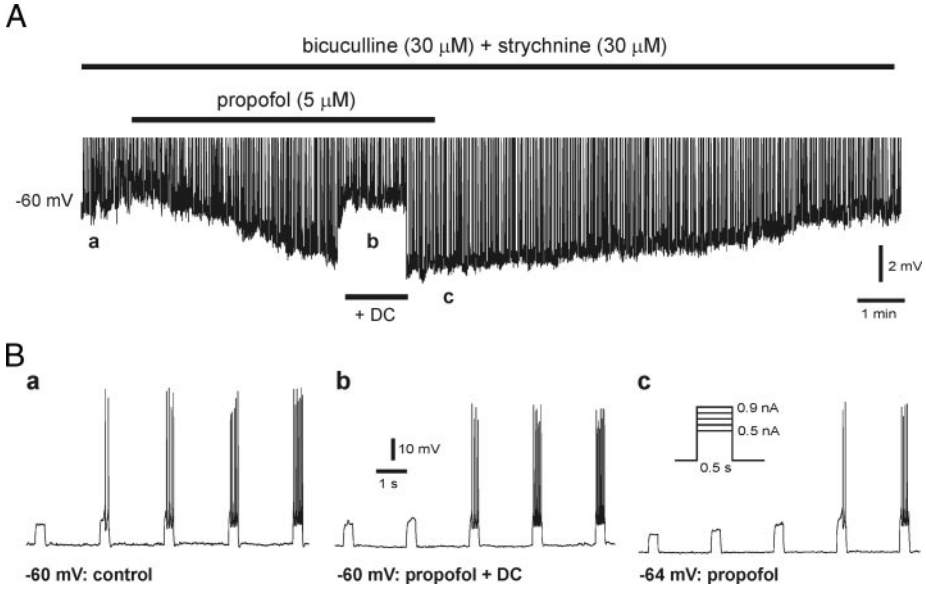

FIG. 6. Propofol causes membrane hyperpolarization and decreased excitability in cortical neurons independent of the $GABA_A$ receptor. *A*: whole cell current-clamp recording of cortical neuron membrane potential before and during bath application of propofol (5 μM) in the continued presence of bicuculline and strychnine (both at 30 μM). At a point near the maximal hyperpolarization induced by propofol (Δ approximately −4 mV), membrane potential was restored to control levels (approximately −60 mV) by using depolarizing DC current injection. Vertical deflections are truncated membrane responses to periodic injections of depolarizing current pulses. *B*: spike firing responses to rectangular depolarizing current pulses (0.5 to 0.9 nA; from points indicated in *A* are expanded. By comparison to control (*a*), depolarizing current pulses of greater magnitude were required to evoke spike firing in the presence of propofol, whether the cell was returned to control membrane potential (*b*) or from the maximal propofol-induced hyperpolarization (*c*).

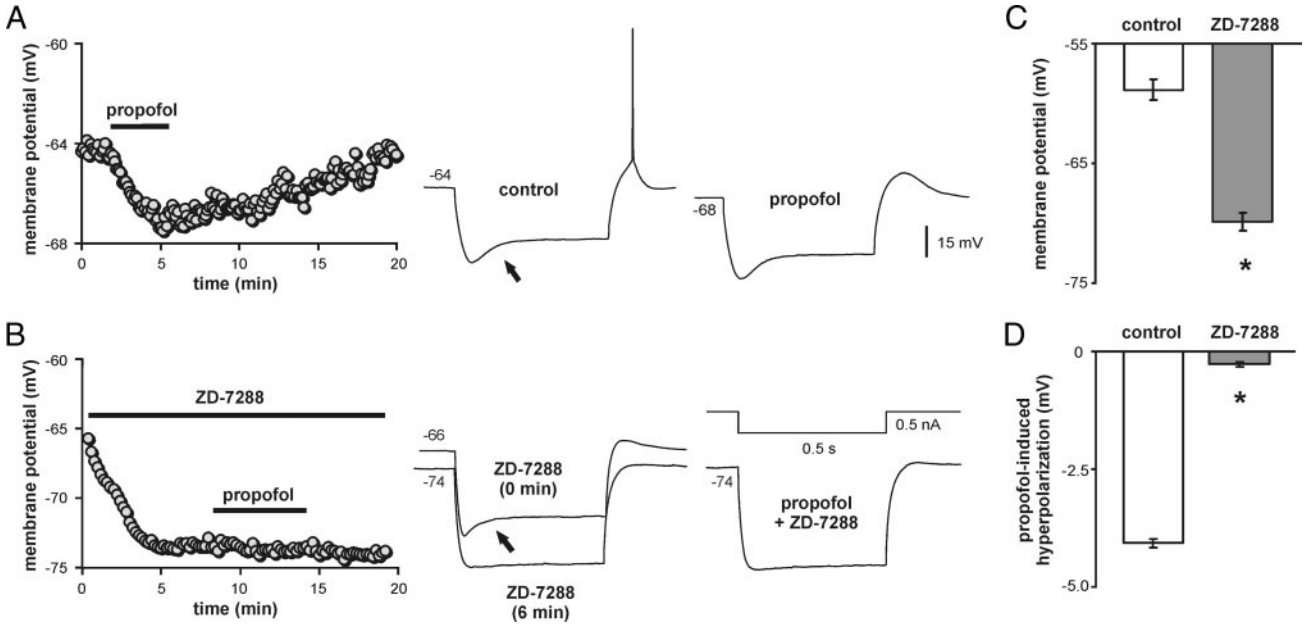

FIG. 7. Inhibition of I_h accounts for membrane hyperpolarization by propofol in cortical neurons. Whole cell current-clamp recordings were performed to test effects of the I_h blocker, ZD-7288 on cortical neuron membrane potential and response to propofol (5 μM) in the continued presence of bicuculline and strychnine (both at 30 μM). *A*: representative time course of membrane hyperpolarization (from −64 to −68 mV) induced by propofol in a cortical neuron recorded without ZD-7288 (*left*); voltage responses to hyperpolarizing current pulses include a "sag" characteristic of I_h activation (→) and a rebound spike that is absent in the presence of propofol (*right*). *B*: time course of membrane potential in a representative cortical neuron recorded with a pipette containing ZD-7288 (50 μM). A progressive hyperpolarization (from −66 to −74 mV) began immediately after obtaining whole cell access (*left*), after which application of propofol had no additional effect on membrane potential. Note that the depolarizing sag (→) and rebound potential that was evident in initial voltage responses to hyperpolarizing current pulses (0 min) disappeared in conjunction with the membrane hyperpolarization (6 min), indicating that I_h was blocked by ZD-7288 at the time of propofol application (*right*). *C*: averaged membrane potential in cortical neurons recorded with normal internal solution and with pipettes containing ZD-7288 (*, $P < 0.05$ by unpaired *t*-test), *D*: averaged propofol-induced hyperpolarization in cortical neurons recorded with normal internal solution and with pipettes containing ZD-7288. (*, $P < 0.001$ by unpaired *t*-test)

cells recorded with ZD-7288 was hyperpolarized ~12 mV relative to control cells (−69.9 ± 1.6 vs. −58.3 ± 3.1 mV; $n = 4$ and $n = 8$, $P < 0.05$; see Fig. 7*C*). The time course of membrane hyperpolarization mirrors the time-dependent, and essentially complete, inhibition of I_h by intracellular ZD-7288 measured under voltage clamp in these neurons (data not shown). In the current-clamp recordings of Fig. 7*B,* the abolition of I_h by ZD-7288 is evident by the loss of the depolarizing voltage sag (→) and rebound potential (compare voltage responses at 0 and 6 min, Fig. 7*B, right*). Consistent with the idea that propofol causes membrane hyperpolarization by inhibition of I_h, we found that propofol had no effect on membrane potential or input resistance when I_h was eliminated by intracellular ZD-7288, (Fig. 7*B*). As is clear from averaged results presented in Fig. 7, *C* and *D,* the I_h blocker ZD-7288 itself caused a significant hyperpolarization (*C*), and it occluded further effects on membrane potential by propofol (*D*).

We found that the I_h blocker Cs^+ (3 mM, bath applied) also caused membrane hyperpolarization (−7.6 ± 1.6 mV) and strongly increased R_N (~110%, from 121.5 ± 11.6 to 250.4 ± 34.0 MΩ; $P < 0.05$) in individual cortical neurons ($n = 4$). Both Cs^+ and ZD-7288 caused nearly identical decreases in I_h and cortical neuron input conductance (~50%) under voltage clamp when the compounds were applied in the bath in the presence of 200 μM Ba^{2+} (data not shown) So, the larger increase in R_N by Cs^+ in these current-clamp experiments, by comparison to ZD-7288, likely reflects two factors: additional block by Cs^+ of inwardly rectifying K^+ currents and partial block of I_h by intracellular ZD-7288 at the earliest time point in the recording. Unfortunately, because cortical neurons became increasingly unstable in the continued presence of Cs^+, even in the presence of TTX and a glutamate receptor blocker (kynurenate, 1 mM), we were unable to test an effect of propofol after blocking I_h with Cs^+.

Overall, these data indicate that I_h contributes a substantial persistent inward current near resting membrane potential in cortical pyramidal neurons, and that inhibition of I_h by propofol can decrease excitability and alter electroresponsive properties of these neurons.

DISCUSSION

In this study, we demonstrated that propofol inhibits a form of I_h with relatively fast activation kinetics ($\tau_f < 200$ ms) that is expressed in mouse cortical pyramidal neurons or rat motoneurons. The inhibition of neuronal I_h by propofol was evident at a clinically relevant concentration (5 μM) and involved a hyperpolarizing shift in voltage dependence of activation, a decrease in maximal available current and a slowing of activation kinetics. On the other hand, propofol had no effect on *V*1/2 of activation or maximal current amplitude of a slower activating form of I_h expressed in thalamocortical relay neurons ($\tau_f > 200$ ms), although kinetic slowing was evident. The different kinetics of I_h observed in mouse cortical and thalamocortical neurons agrees with prior electrophysiological work (Santoro et al. 2000); it is also consistent with greater expression of fast-activating HCN1 subunits in mouse cortex (particularly in layer V pyramidal neurons) and with

higher densities of slower activating HCN2 and HCN4 subunits in thalamic relay nuclei (Santoro et al. 2000). Accordingly, propofol modulated cloned homomeric HCN1 or heteromeric HCN1–HCN2 channel currents in ways reminiscent of its effects on I_h in cortical neurons, causing a negative shift in *V*1/2, decreasing maximal current amplitude and slowing activation kinetics. Also consistent with actions of the anesthetic on native I_h in thalamocortical neurons, we found that cloned HCN2 homomeric channels were relatively insensitive to propofol, showing only kinetic slowing with no change in voltage dependence or maximal amplitude. Propofol suppressed excitability in cortical neurons, causing membrane hyperpolarization and decreasing action potential discharge. These actions of propofol were due to inhibition of I_h because they persisted when $GABA_A$ and glycine receptors were blocked but were completely occluded when I_h was inhibited by ZD-7288. In sum, these results indicate that modulation of I_h by propofol in cortical pyramidal cells and motoneurons, and perhaps in other HCN1-expressing cells, may contribute to its GABA-independent anesthetic and/or anticonvulsant actions (Higuchi et al. 2003).

Any suggestion of a role for I_h inhibition in the clinical actions of propofol presupposes modulation of the channels over a concentration range that is achieved clinically. In this respect, circulating concentrations of propofol at which 50% of patients fail to respond to verbal command and skin incision are 3.3 μg/ml (18 μM) and 15.2 μg/ml (85 μM), respectively (Smith et al. 1994). Because >95% of propofol is bound to serum proteins, free fractions of propofol that produce these anesthetic actions are expected to range from 1 to 4.5 μM, but may be as high as 10 μM (Shyr et al. 1995). We showed that inhibitory effects of propofol on cortical I_h and on HCN1 subunit-containing channels occur within this clinically relevant concentration range, with near maximal effects at 5 μM. If access of the drug to the slice is limited, as has been suggested (Bieda and MacIver 2004; Gredell et al. 2004), the actual effective concentration of propofol at the channel may be even lower than the bath concentrations we report.

We found a strong inhibition of I_h by propofol in pyramidal neurons of the neocortex similar to that previously reported in CA1 hippocampal pyramidal neurons, although higher concentrations of propofol (50 μM to 1 mM) were necessary for propofol actions on hippocampal I_h (Funahashi et al. 2001, 2004; Higuchi et al. 2003). The reason for this different propofol sensitivity in pyramidal neurons from neocortex and hippocampus, despite generally similar HCN expression and I_h properties in the two cell types, remains to be determined. As with layer V neocortical neurons, CA1 hippocampal pyramidal neurons appear to express HCN1 predominantly, along with HCN2, and a corresponding native I_h with fast activation kinetics (fast activation τ<100 ms at approximately −100 mV) (Santoro et al. 2000). Given joint expression of both HCN1 and HCN2 subunits in cortical and hippocampal pyramidal neurons, it is likely that I_h in these cells includes a contribution from homomeric HCN channels as well as heteromeric HCN1–HCN2 channels. Importantly, we showed that these heteromeric HCN1–HCN2 channels also produce currents with fast kinetics that are modulated by propofol.

We found that propofol caused membrane hyperpolarization near resting membrane potential (i.e., at −60 mV) and decreased excitability in neocortical neurons in a ZD-7288-sensitive manner, as also observed in hippocampal CA1 pyramidal neurons (Higuchi et al. 2003). This ZD-7288-sensitive action of propofol at relatively depolarized membrane potentials likely involves inhibition of a tonic component of I_h because we find that only ~5% of the voltage- and time-dependent current component is available at −60 mV (e.g., see Fig. 2*A*). Consistent with this, we showed that propofol can robustly inhibit tonic currents from HCN1 subunit-containing channels. In addition, it is possible that inhibition of dendritic I_h by propofol could enhance temporal summation of synaptic inputs in those neurons, especially those impinging on distal dendrites where I_h channels are most dense (Magee 2000; Migliore and Shepherd 2002). Other ionic mechanisms likely also contribute to effects of propofol on cortical neuron excitability. For example, propofol can inhibit apamin-sensitive calcium-activated K^+ currents (Ying and Goldstein 2005), and it enhances synaptic as well as tonically active $GABA_A$ currents in neocortical and hippocampal neurons (Bieda and MacIver 2004; Orser et al. 1994). So, it seems that multiple ion channel targets—intrinsic and synaptic, acting tonically and phasically—could contribute to complex integrated actions of propofol in cortical neurons and elsewhere.

As mentioned in the preceding text (see INTRODUCTION), although some anesthetic actions of propofol certainly involve enhancement of $GABA_A$ receptor (Jurd et al. 2003), existing pharmacological and genetic evidence leave open the possibility that other targets may also be important. In this respect, a role for HCN channels in hypnotic or amnestic effects of general anesthetics is intriguing. Thalamocortical circuits are implicated in the sleep-like actions of anesthetics (Alkire et al. 2000) and inhibition of I_h in thalamic relay neurons and cortical neurons is associated with sleep-like rhythmic network activity (Pape 1996; Pape and McCormick 1989). Our data suggest that any induction by propofol of a sleep-like state that involves actions on I_h within thalamocortical circuits will engage primarily the cortical neuron component, where its actions on I_h were most prominent. However, it is also possible that the propofol-induced slowing of I_h activation kinetics we observed in cortical and thalamocortical relay neurons could also modulate rhythmic thalamocortical activity. In addition, I_h underlies a "pacemaker" current for generating the theta-like oscillations in entorhinal pyramidal neurons that provide a synchronizing mechanism important in memory formation (Dickson et al. 2000). Inhibition of cortical neuronal I_h by propofol could disrupt such network coherence and thereby contribute to amnestic actions of the drug.

In conclusion, we have found that propofol inhibits the neuronal pacemaker current, I_h, in cortical pyramidal neurons at clinically relevant concentrations. These currents contribute to setting membrane potential and input resistance, they modulate dendritic integration, and they are crucial for multiple cortical rhythms (Pape 1996). These data are consistent with accumulating evidence that general anesthetics do not simply provide widespread suppression of neuronal excitability. Rather it is likely that anesthetic drugs target multiple distinct types of ion channel at specific sites where they commandeer certain aspects of normal neuronal activity patterns to generate the anesthetic state. The precise contribution of HCN channel inhibition to overall anesthetic actions in cortical neurons will require modeling in simulated networks or experiments in animals with targeted disruption of HCN subunits.

ACKNOWLEDGMENTS

We thank Drs. B. Santoro and S. A. Siegelbaum for generous gifts of HCN channel constructs; we also thank Drs. G. Kamatchi and H. Fang for kindly providing *Xenopus* oocytes.

GRANTS

This work was supported by National Institute of General Medical Sciences Grant GM-66181.

REFERENCES

Aghajanian GK and Rasmussen K. Intracellular studies in the facial nucleus illustrating a simple new method for obtaining viable motoneurons in adult rat brain slices. *Synapse* 3: 331–338, 1989.

Alkire MT, Haier RJ, and Fallon JH. Toward a unified theory of narcosis: brain imaging evidence for a thalamocortical switch as the neurophysiologic basis of anesthetic-induced unconsciousness. *Conscious Cogn* 9: 370–386, 2000.

Bieda MC and MacIver MB. Major role for tonic $GABA_A$ conductances in anesthetic suppression of intrinsic neuronal excitability. *J Neurophysiol* 92: 1658–1667, 2004.

Biel M, Ludwig A, Zong X, and Hofmann F. Hyperpolarization-activated cation channels: a multi-gene family. *Rev Physiol Biochem Pharmacol* 136: 165–181, 1999.

Bosmith RE, Briggs I, and Sturgess NC. Inhibitory actions of Zeneca-ZD7288 on whole-cell hyperpolarization-activated inward current (I_f) in guinea-pig dissociated sinoatrial node cells. *Br J Pharmacol* 110: 343–349, 1993.

Chen C, Wang C, and Siegelbaum SA. Properties of hyperpolarization-activated pacemaker current defined by coassembly of HCN1 and HCN2 subunits and basal modulation by cyclic nucleotide. *J Gen Physiol* 117: 491–503, 2001.

Chen J, Mitcheson JS, Tristani-Firouzi M, Lin M, and Sanguinetti MC. The S4-S5 linker couples voltage sensing and activation of pacemaker channels. *Proc Natl Acad Sci USA* 98: 11277–11282, 2001.

Chen X, Sirois JE, Lei Q, Talley EM, Lynch C, and Bayliss DA. HCN subunit-specific and cAMP-modulated effects of anesthetics on neuronal pacemaker currents. *J Neurosci* 25: 5803–5814, 2005.

Decher N, Chen J, and Sanguinetti MC. Voltage-dependent gating of hyperpolarization-activated, cyclic nucleotide-gated pacemaker channels: molecular coupling between the S4-S5 and C-linkers. *J Biol Chem* 279: 13859–13865, 2004.

Dickson CT, Magistretti J, Shalinsky M, Hamam B, and Alonso A. Oscillatory activity in entorhinal neurons and circuits. Mechanisms and function. *Ann NY Acad Sci* 911: 127–150, 2000.

Franz O, Liss B, Neu A, and Roeper J. Single-cell mRNA expression of HCN1 correlates with a fast gating phenotype of hyperpolarization-activated cyclic nucleotide-gated ion channels (I_h) in central neurons. *Eur J Neurosci* 12: 2685–2693, 2000.

Funahashi M, Higuchi H, Miyawaki T, Shimada M, and Matsuo R. Propofol suppresses a hyperpolarization-activated inward current in rat hippocampal CA1 neurons. *Neurosci Lett* 311: 177–180, 2001.

Funahashi M, Mitoh Y, and Matsuo R. The sensitivity of hyperpolarization-activated cation current (I_h) to propofol in rat area postrema neurons. *Brain Res* 1015: 198–201, 2004.

Gredell JA, Turnquist PA, MacIver MB, and Pearce RA. Determination of diffusion and partition coefficients of propofol in rat brain tissue: implications for studies of drug action in vitro. *Br J Anaesth* 93: 810–817, 2004.

Higuchi H, Funahashi M, Miyawaki T, Mitoh Y, Kohjitani A, Shimada M, and Matsuo R. Suppression of the hyperpolarization-activated inward current contributes to the inhibitory actions of propofol on rat CA1 and CA3 pyramidal neurons. *Neurosci Res* 45: 459–472, 2003.

Jurd R, Arras M, Lambert S, Drexler B, Siegwart R, Crestani F, Zaugg M, Vogt KE, Ledermann B, Antkowiak B, and Rudolph U. General anesthetic actions in vivo strongly attenuated by a point mutation in the $GABA_A$ receptor β3 subunit. *FASEB J* 17: 250–252, 2003.

Kaupp UB and Seifert R. Molecular diversity of pacemaker ion channels. *Annu Rev Physiol* 63: 235–257, 2001.

Little HJ, Clark A, and Watson WP. Investigations into pharmacological antagonism of general anaesthesia. *Br J Pharmacol* 129: 1755–1763, 2000.

Ludwig A, Budde T, Stieber J, Moosmang S, Wahl C, Holthoff K, Langebartels A, Wotjak C, Munsch T, Zong X, Feil S, Feil R, Lancel M, Chien KR, Konnerth A, Pape HC, Biel M, and Hofmann F. Absence epilepsy and sinus dysrhythmia in mice lacking the pacemaker channel HCN2. *EMBO J* 22: 216–224, 2003.

Ludwig A, Zong XG, Jeglitsch M, Hofmann F, and Biel M. A family of hyperpolarization-activated mammalian cation channels. *Nature* 393: 587–591, 1998.

Macri V and Accili EA. Structural elements of instantaneous and slow gating in hyperpolarization-activated cyclic nucleotide-gated channels. *J Biol Chem* 279: 16832–16846, 2004.

Magee JC. Dendritic integration of excitatory synaptic input. *Nat Rev Neurosci* 1: 181–190, 2000.

Migliore M and Shepherd GM. Emerging rules for the distributions of active dendritic conductances. *Nat Rev Neurosci* 3: 362–370, 2002.

Mistrik P, Mader R, Michalakis S, Weidinger M, Pfeifer A, and Biel M. The murine HCN3 gene encodes a hyperpolarization-activated cation channel with slow kinetics and unique response to cyclic nucleotides. *J Biol Chem* 280: 27056–27061, 2005.

Monteggia LM, Eisch AJ, Tang MD, Kaczmarek LK, and Nestler EJ. Cloning and localization of the hyperpolarization-activated cyclic nucleotide-gated channel family in rat brain. *Brain Res Mol Brain Res* 81: 129–139, 2000.

Moosmang S, Biel M, Hofmann F, and Ludwig A. Differential distribution of four hyperpolarization-activated cation channels in mouse brain. *Biol Chem* 380: 975–980, 1999.

Much B, Wahl-Schott C, Zong XG, Schneider A, Baumann L, Moosmang S, Ludwig A, and Biel M. Role of subunit heteromerization and N-linked glycosylation in the formation of functional hyperpolarization-activated cyclic nucleotide-gated channels. *J Biol Chem* 278: 43781–43786, 2003.

Notomi T and Shigemoto R. Immunohistochemical localization of I_h channel subunits, HCN1-4, in the rat brain. *J Comp Neurol* 471: 241–276, 2004.

Ohmori H, Sato Y, and Namiki A. The anticonvulsant action of propofol on epileptiform activity in rat hippocampal slices. *Anesth Analg* 99: 1095–1101, 2004.

Orser BA, Wang LY, Pennefather PS, and Macdonald JF. Propofol modulates activation and desensitization of $GABA_A$ receptors in cultured murine hippocampal-neurons. *J Neurosci* 14: 7747–7760, 1994.

Pape HC. Queer current and pacemaker: The hyperpolarization-activated cation current in neurons. *Annu Rev Physiol* 58: 299–327, 1996.

Pape HC and McCormick DA. Noradrenaline and serotonin selectively modulate thalamic burst firing by enhancing a hyperpolarization-activated cation current. *Nature* 340: 715–718, 1989.

Proenza C, Angoli D, Agranovich E, Macri V, and Accili EA. Pacemaker channels produce an instantaneous current. *J Biol Chem* 277: 5101–5109, 2002.

Rudolph U and Antkowiak B. Molecular and neuronal substrates for general anaesthetics. *Nat Rev Neurosci* 5: 709–720, 2004.

Santoro B, Chen S, Luthi A, Pavlidis P, Shumyatsky GP, Tibbs GR, and Siegelbaum SA. Molecular and functional heterogeneity of hyperpolarization-activated pacemaker channels in the mouse CNS. *J Neurosci* 20: 5264–5275, 2000.

Santoro B, Grant SGN, Bartsch D, and Kandel ER. Interactive cloning with the SH3 domain of N-src identifies a new brain specific ion channel protein, with homology to Eag and cyclic nucleotide-gated channels. *Proc Natl Acad Sci USA* 94: 14815–14820, 1997.

Santoro B and Tibbs GR. The HCN gene family: molecular basis of the hyperpolarization-activated pacemaker channels. *Ann NY Acad Sci* 868: 741–764, 1999.

Shyr MH, Tsai TH, Tan PPC, Chen CF, and Chan SHH. Concentration and regional distribution of propofol in brain and spinal-cord during propofol anesthesia in the rat. *Neurosci Lett* 184: 212–215, 1995.

Sirois JE, Lynch C, and Bayliss DA. Convergent and reciprocal modulation of a leak K^+ current and I_h by an inhalational anaesthetic and neurotransmitters in rat brainstem motoneurons. *J Physiol* 541: 717–729, 2002.

Sirois JE, Pancrazio JJ, Lynch C, and Bayliss DA. Multiple ionic mechanisms mediate inhibition of rat motoneurones by inhalation anaesthetics. *J Physiol* 512: 851–862, 1998.

Smith C, Mcewan AI, Jhaveri R, Wilkinson M, Goodman D, Smith LR, Canada AT, and Glass PSA. The interaction of fentanyl on the CP_{50} of propofol for loss of consciousness and skin incision. *Anesthesiology* 81: 820–828, 1994.

Sonner JM, Antognini JF, Dutton RC, Flood P, Gray AT, Harris RA, Homanics GE, Kendig J, Orser B, Raines DE, Rampil IJ, Trudell J, Vissel B, and Eger EI. Inhaled anesthetics and immobility: mechanisms, mysteries, and minimum alveolar anesthetic concentration. *Anesth Analg* 97: 718–740, 2003a.

Sonner JM, Zhang Y, Stabernack C, Abaigar W, Xing YL, and Laster MJ. $GABA_A$ receptor blockade antagonizes the immobilizing action of propofol but not ketamine or isoflurane in a dose-related manner. *Anesth Analg* 96: 706–712, 2003b.

Talley EM, Lei QB, Sirois JE, and Bayliss DA. TASK-1, a two-pore domain K^+ channel, is modulated by multiple neurotransmitters in motoneurons. *Neuron* 25: 399–410, 2000.

Trapani G, Altomare C, Sanna E, Biggio G, and Liso G. Propofol in anesthesia. mechanism of action, structure-activity relationships, and drug delivery. *Curr Med Chem* 7: 249–271, 2000.

Ulens C and Tytgat J. Functional heteromerization of HCN1 and HCN2 pacemaker channels. *J Biol Chem* 276: 6069–6072, 2001.

Ying SW and Goldstein PA. Propofol-block of SK channels in reticular thalamic neurons enhances GABAergic inhibition in relay neurons. *J Neurophysiol* 93: 1935–1948, 2005.